Gallic acid causes inactivating phosphorylation of cdc25A/cdc25C-cdc2 via ATM-Chk2 activation, leading to cell cycle arrest, and induces apoptosis in human prostate carcinoma DU145 cells

Chapla Agarwal,[1,2] Alpna Tyagi,[1] and Rajesh Agarwal[1,2]

[1]Department of Pharmaceutical Sciences, School of Pharmacy; and [2]University of Colorado Cancer Center, University of Colorado Health Sciences Center, Denver, Colorado

Abstract

We recently reported that gallic acid is a major active agent responsible for grape seed extract activity in DU145 human prostate carcinoma cells. The present study was conducted to examine its efficacy and associated mechanism. Gallic acid treatment of DU145 cells resulted in a strong cell growth inhibition, cell cycle arrest, and apoptotic death in a dose- and time-dependent manner, together with a decrease in cyclin-dependent kinases and cyclins but strong induction in Cip1/p21. Additional mechanistic studies showed that gallic acid induces an early Tyr^{15} phosphorylation of cell division cycle 2 (cdc2). Further upstream, gallic acid also induced phosphorylation of both cdc25A and cdc25C via ataxia telangiectasia mutated (ATM)-checkpoint kinase 2 (Chk2) activation as a DNA damage response evidenced by increased phosphohistone 2AX (H2A.X) that is phosphorylated by ATM in response to DNA damage. Time kinetics of ATM phosphorylation, together with those of H2A.X and Chk2, was in accordance with an inactivating phosphorylation of cdc25A and cdc25C phosphatases and cdc2 kinase, suggesting that gallic acid increases cdc25A/C-cdc2 phosphorylation and thereby inactivation via ATM-Chk2 pathway following DNA damage that induces cell cycle arrest. Caffeine, an ATM/ataxia telangiectasia-rad3-related inhibitor, reversed gallic acid–caused ATM and H2A.X phosphorylation and cell cycle arrest, supporting the role of ATM pathway in gallic acid–induced cell cycle arrest. Additionally, gallic acid caused caspase-9, caspase-3, and poly(ADP)ribose polymerase cleavage, but pan-caspase inhibitor did not reverse apoptosis, suggesting an additional caspase-independent apoptotic mechanism. Together, this is the first report identifying gallic acid efficacy and associated mechanisms in an advanced and androgen-independent human prostate carcinoma DU145 cells, suggesting future *in vivo* efficacy studies with this agent in preclinical prostate cancer models. [Mol Cancer Ther 2006;5(12):3294–302]

Introduction

Prostate cancer is the second most common male malignancy and leading cause of deaths in men in the United States and Europe. The management and treatment of hormone-refractory prostate cancer (advanced stage) is a major problem, which increases morbidity and mortality in prostate cancer patients. Statistical predictions for 2006 show an estimated 234,460 new cases of prostate cancer with 27,350 deaths in the United States alone (1). Because the advanced-stage prostate cancer growth and development become independent of androgen and renders androgen ablation therapy ineffective, prostate cancer control through chemoprevention or intervention is highly desirable, which deals with suppression or reversal of both premalignant and malignant lesions by natural or synthetic agents (2–4). It is also important to emphasize here that the abnormal expression of growth factors and receptors, which is often associated with prostatic-intraepithelial neoplasia and invasive prostate cancer, leads to autocrine and paracrine loops for both mitogenic and antiapoptotic signaling leading to uncontrolled cell cycle progression followed by a growth advantage to cancer cells together with a loss of their apoptotic cell death (2–4). Accordingly and consistent with the above notion, the antiproliferative and apoptotic effects of nontoxic dietary agents could be of additional significance for the prevention, control, and/or management of prostate cancer, specifically that at an advanced and an androgen-independent stage of the malignancy. In this regard, various phytochemicals present in diet and those consumed as supplement are gaining increased attention in cancer chemoprevention research, including prostate cancer, focusing on both efficacy studies and associated mechanisms (refs. 2–6 and references therein).

Grape seed extract, also termed as grape seed polyphenols or procyanidins, is one such dietary supplement marketed in the United States as ''grape seed extract'' with 95% standardized procyanidins due to its several health

Received 8/10/2006; revised 10/6/2006; accepted 10/30/2006.

Grant support: National Cancer Institute/NIH grant CA91883 (C. Agarwal).

The costs of publication of this article were defrayed in part by the payment of page charges. This article must therefore be hereby marked advertisement in accordance with 18 U.S.C. Section 1734 solely to indicate this fact.

Requests for reprints: Chapla Agarwal, Department of Pharmaceutical Sciences, School of Pharmacy, University of Colorado Health Sciences Center, 4200 East Ninth Avenue, Box C238, Denver, CO 80262. Phone: 303-315-1382; Fax: 303-315-6281. E-mail: Chapla.Agarwal@uchsc.edu

doi:10.1158/1535-7163.MCT-06-0483

benefits (7, 8). In addition to grape seeds, procyanidins are a diverse group of polyphenolic compounds that are also abundant in blackjack oak, horse chestnut, witch hazel, and hawthorn, as well as in apples, berries, barley, bean hulls, chocolate, rhubarb, rose hips, and sorghum (refs. 7–9 and references therein).

About the anticancer and cancer chemopreventive effects of grape seed extract, it inhibits the growth of human breast, lung, and gastric cancer cells but enhances the growth and viability of normal human gastric mucosal and normal murine macrophage cells (10). Our studies have shown that grape seed extract inhibits growth, induces cell cycle arrest, and causes apoptotic death of human breast carcinoma MDA-MB468, prostate carcinoma DU145, and LNCaP cells in culture (11–14). With regard to its anticarcinogenic effects in animal models, oral feeding of grape seed extract or procyanidin-rich fraction from grape seed extract has been shown to prevent azoxymethane-induced aberrant crypt foci formation in rats (15, 16), and that topical application of grape seed extract significantly prevents chemical and UVB radiation–induced skin tumorigenesis (17–19). With regard to the *in vivo* efficacy of grape seed extract against prostate cancer, we recently reported that oral feeding of grape seed extract strongly suppresses *in vivo* growth of advanced human prostate cancer DU145 xenograft in athymic nude mice (20). Together, these studies have convincingly documented the anticancer and chemopreventive efficacy of grape seed extract against various epithelial cancers, including prostate cancer, and have suggested the presence of biologically active phytochemicals in the crude mixture of grape seed extract.

In an effort to isolate and identify active compounds in grape seed extract, we recently found that gallic acid (Fig. 1) substantially contributes to the biological effects of grape seed extract in DU145 cells toward both cell growth inhibition and apoptotic cell death (21). The present study, therefore, was designed to examine efficacy and associated mechanism of gallic acid in advanced human prostate carcinoma DU145 cells; our objectives were (*a*) to study the effect of gallic acid on the growth and survival, cell cycle progression, and apoptotic death of DU145 cells; and (*b*) to study the molecular mechanisms of the biological effects of gallic acid. Our results provide the first evidence for the activation of ataxia telangiectasia-mutated (ATM)–checkpoint kinase (Chk) signaling as a central mechanism of gallic acid–induced cell cycle arrest in its biological effects in DU145 cells.

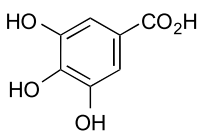

gallic acid (GA)

Figure 1. Chemical structure of gallic acid (*GA*).

Materials and Methods

Cell Lines and Reagents

The human prostate carcinoma DU145 cell line was from American Type Culture Collection (Manassas, VA). Cells were cultured in RPMI 1640 with 10% fetal bovine serum (Hyclone, Logan, UT) and 1% penicillin-streptomycin under standard culture conditions (37°C, 95% humidified air and 5% CO_2). RPMI 1640 and other culture materials were from Life Technologies, Inc. (Gaithersburg, MD). Gallic acid used in the present study was from Sigma-Aldrich Chemical Company (St. Louis, MO). The primary antibodies for cyclin-dependent kinase (CDK) 4, CDK2, CDK6; cyclins D1, D3, E, A, B1; and cell division cycle 25 A (cdc25A) were from Santa Cruz Biotechnology (Santa Cruz, CA). Antibody for CDK inhibitor Kip1/p27 was from Neomarkers (Fremont, CA); antibody for phospho-cdc25A was from Abcam (Cambridge, MA); and antibody for actin was from Sigma-Aldrich. Primary antibodies for phospho- and total cdc25C and cdc2; Chk2 and Chk1; total cdc25B; and cleaved caspase-9, caspase-3, and poly(ADP)ribose polymerase were from Cell Signaling, Inc. (Beverly, MA). Antibody for phospho-ATM was from Rockland Immunochemicals (Gilbertsville, PA), and antibodies for Cip1/p21 and phospho-H2A.X were from Upstate Biotechnologies (Lake Placid, NY). Antibody for ataxia telangiectasia-rad3-related (ATR) was from Novus (Littleton, CO). Secondary anti-mouse antibody and enhanced chemiluminescence (ECL) detection system were from Amersham (Arlington Heights, IL). For all the gallic acid treatments, a 1,000-fold concentrated stock solution was prepared in DMSO and diluted directly into the medium immediately before the treatment of the cells.

Cell Growth and Death Assays

DU145 cells were plated at 1×10^5/60-mm plates under standard culture condition, and after 24 h, cells were fed with fresh medium and treated with DMSO alone (control) or varying doses of gallic acid (10–50 μmol/L, final concentrations in medium) dissolved in DMSO for different time points (24–72 or 6–24 h). The DMSO concentration was the same for all treatments and did not exceed 0.1% (v/v). After the desired treatment, cells were collected with brief trypsinization, washed with ice-cold PBS, and counted in duplicate using a hemocytometer. Trypan blue dye exclusion was used to determine cell viability.

Flow Cytometry for Cell Cycle Analysis

DU145 cells at 60% confluency were treated with either DMSO alone or 50 μmol/L gallic acid in DMSO for 6, 12, and 24 h. Alternatively, cells were treated with DMSO, 50 μmol/L gallic acid, and 2.5 mmol/L caffeine without, or followed 2 h later with, 50 μmol/L gallic acid for 24 h. Following these treatments, the medium was aspirated, cells were trypsinized, and cell pellets were collected. Approximately 0.5×10^5 cells in 0.5 mL of saponin-propidium iodide solution (0.3% saponin, 25 μg/mL propidium iodide, 0.1 mmol/L EDTA, and 10 μg/mL RNase in PBS) were incubated at 4°C for 24 h in the dark. Cell cycle distribution was then analyzed by flow cytometry using the fluorescence-activated cell sorting analysis

core service of the University of Colorado Cancer Center (Denver, CO).

Quantitative Apoptotic Cell Death Assay

To quantify gallic acid–induced apoptotic death of DU145 cells, Annexin V and propidium iodide staining was done followed by flow cytometry, as recently described (21). Briefly, after treatment with DMSO or 50 μmol/L gallic acid in DMSO as a function of time for 6, 12, and 24 h, cells were collected by brief trypsinization and washed with PBS twice. Cells were then subjected to Annexin V and propidium iodide staining using Vybrant Apoptosis Assay Kit 2 (Molecular Probes, Eugene, OR) following the step-by-step protocol provided by the manufacturer. The kit contains recombinant Annexin V conjugated to fluorophores and the Alexa Fluor 488 dye, providing maximum sensitivity. After staining, flow cytometry was done for the quantification of apoptotic cells. In the caspase inhibitor study, cells were pretreated with 50 μmol/L pan-caspase inhibitor ZVAD.fmk (Enzyme Systems Products, Livermore, CA), 2 h before treatment with 50 μmol/L gallic acid.

Immunoblot Analysis

Cells were treated with DMSO or 50 μmol/L gallic acid in DMSO for the desired time periods. In caffeine and gallic acid combination studies, cells were treated with caffeine (2.5 mmol/L) 2 h before gallic acid treatment. In pan-caspase inhibitor study, cells were treated with ZVAD.fmk (50 μmol/L) 2 h before gallic acid treatment at 50 μmol/L dose. Following desired treatments, cell lysates were prepared in nondenaturing lysis buffer [10 mmol/L Tris-HCl (pH 7.4), 150 mmol/L NaCl, 1% Triton X-100, 1 mmol/L EDTA, 1 mmol/L EGTA, 0.3 mmol/L phenylmethylsulfonyl fluoride, 0.2 mmol/L sodium orthovanadate, 0.5% NP40, 5 units/mL aprotinin]. Briefly, medium was aspirated and cells were washed with ice-cold PBS twice, followed by incubation in lysis buffer for 10 min on ice. Then, cells were scraped and kept on ice for 30 min, and finally cell lysates were cleared by centrifugation at 4°C for 30 min at 14,000 rpm. Protein concentrations in lysates were determined using Bio-Rad detergent-compatible protein assay kit (Bio-Rad Laboratories, Hercules, CA) by the Lowry method.

For immunoblot analysis, total cell lysates were denatured in 2× sample buffer; samples were subjected to SDS-PAGE on 4%, 12%, or 16% Tris-glycine gels; and separated proteins were transferred onto membrane by Western blotting. Membranes were blocked with blocking buffer for 1 h at room temperature and probed with primary antibodies against desired molecules overnight at 4°C followed by peroxidase-conjugated appropriate secondary antibody for 1 h at room temperature and ECL detection. In each case, blots were subjected to multiple exposures on the film to make sure that the band density is in the linear range. The bands were scanned with Adobe Photoshop 6.0 (Adobe Systems, Inc., San Jose, CA), and, as needed, the mean density of each band was analyzed by the Scion Image program (NIH, Bethesda, MD).

Statistical Analysis

Statistical significance of differences between control and treated samples were calculated by Student's t test (SigmaStat 2.03). $P < 0.05$ was considered significant. All the results shown are representative of at least two to four independent experiments with reproducible findings.

Results

Effect of Gallic Acid on Cell Growth and Viability, Cell Cycle Progression, and Apoptotic Death

To examine the biological effects of gallic acid, DU145 cells were treated with varying doses of gallic acid (10, 25, 40, and 50 μmol/L) for 24, 48, and 72 h, and both cell growth inhibition and cell death were assayed. The results of this experiment showed that gallic acid causes both cell-growth inhibition and cell death only at its two higher doses, 40 and 50 μmol/L, without any time-dependent response (data not shown). Based on these pilot observations, an early time-response study was next done to assess the effect of gallic acid at 40 and 50 μmol/L doses, which caused strong cell growth inhibition (Fig. 2A) and cell death induction (Fig. 2B) mostly in a dose-dependent, but not time-dependent (except 24 h), manner. Compared with DMSO-treated control cells, 50 μmol/L gallic acid treatment for 24 h resulted in 62% inhibition ($P < 0.001$) of cell growth (Fig. 2A) and caused 39% ($P < 0.001$) cell death (Fig. 2B). Based on these results, we selected the 50 μmol/L dose and next assessed whether the growth-inhibitory and cell death effects of gallic acid are accompanied by its effect on cell cycle progression and/or apoptotic cell death.

Gallic acid showed statistically significant cell cycle arrest at 50 μmol/L dose following its treatment for 6, 12, and 24 h (Fig. 2C). At early time points of 6 and 12 h, compared with vehicle controls, it caused an arrest in both S (32% versus 40% and 20% versus 38%, respectively, $P < 0.001$) and G_2-M (20% versus 23%, $P = 0.001$ and 17% versus 22%, $P = 0.005$, respectively) phases, which were at the expense of a strong decrease in G_1-phase cell population (Fig. 2C). When similar gallic acid treatment was done for 24 h, compared with vehicle control showing 15% cells in G_2-M phase, 28% of the gallic acid–treated cells showed their accumulation in G_2-M phase accounting for almost 1.87-fold increase ($P = 0.004$) compared with control without any change in S-phase population (Fig. 2C). The G_2-M accumulation of cells at this time point was only at the expense of a decrease in G_1-phase cell population (Fig. 2C). In other studies assessing whether gallic acid also causes apoptotic cell death, as shown in Fig. 2D, its treatment at 50 μmol/L dose for 6, 12, and 24 h resulted in a strong and statistically significant apoptotic cell death. The early time points of gallic acid treatment resulted in almost 3-fold increase ($P < 0.001$ and $P = 0.012$) in apoptotic cells compared with vehicle controls (Fig. 2D); however, a similar gallic acid treatment for 24 h resulted in 39.2% apoptotic cells compared with 5.4% in control accounting for 7.3-fold increase ($P < 0.001$) in apoptotic cells by gallic acid versus control (Fig. 2D). In other studies, 40 μmol/L

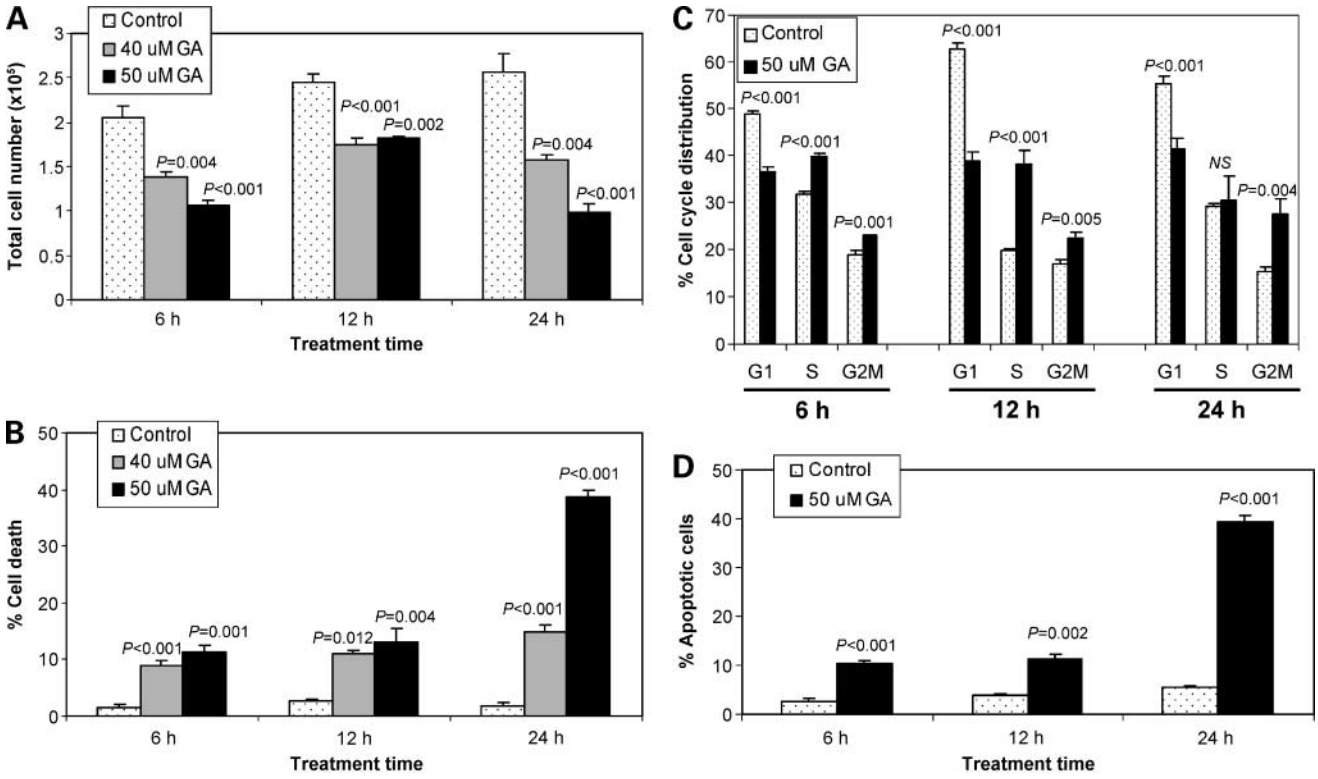

Figure 2. Gallic acid causes growth inhibition, death, cell cycle arrest, and apoptosis in DU145 cells. Cells (1×10^5) were plated in 60-mm dishes, and after 24 h were treated with DMSO (control) or different concentrations (40 and/or 50 μmol/L) of gallic acid for 6, 12, and 24 h. At the end of these treatments, cells were harvested and counted for total cell number (**A**), percentage of cell death (**B**), cell cycle phase distribution by saponin/propidium iodide staining followed by fluorescence-activated cell sorting analysis (**C**), or percentage of apoptotic cells by Annexin V/propidium iodide staining and fluorescence-activated cell sorting analysis (**D**), as detailed in Materials and Methods. *Columns,* mean of three independent samples; *bars,* SE. Data were reproducible in additional independent experiment(s). *NS,* not significant.

gallic acid also showed a moderate S-phase arrest in the cell cycle progression and caused 6% to 16% apoptotic cell death at 6 to 24 h of treatment (data not shown). Together, the results shown in Fig. 2 clearly show the biological effects of gallic acid on DU145 cell growth inhibition and death, as well as cell cycle arrest and apoptosis induction. Accordingly, studies were next done to examine the mechanism of cell cycle arrest by gallic acid in DU145 cells.

Effect of Gallic Acid on CDKs, Cyclins, and CDK Inhibitor Levels

Because gallic acid treatment of cells caused cell cycle arrest as early as 6 h after its treatment that sustained even at 24 h, a time kinetics study starting at 3 h was done to examine the effect of 50 μmol/L gallic acid on the protein levels of cell cycle regulatory molecules. In terms of the levels of CDKs, which drive the cell cycle by the phosphorylation of Rb, making transcription factor E2Fs free (2, 4), gallic acid caused a decrease in CDK4, CDK6, and CDK2 protein albeit at different levels following different treatment times. However, no effect was evidenced following 3-h gallic acid treatment (Fig. 3A). One of the two important regulators of CDKs is their regulatory subunit cyclins that bind to and positively regulate CDK activity (2, 4), and, therefore, we next assessed the effect of gallic acid on cyclin levels. As shown in Fig. 3A, gallic acid treatment of cells for varying time periods also resulted in a decrease in the protein levels of various cyclins. Interestingly, the levels of cyclin D1 and cyclin D3 decreased at early time points of gallic acid treatment, but those of cyclin A and cyclin B1 at later time points of 12 and 24 h, without any effect on cyclin E levels; the maximum gallic acid effect was evidenced on cyclin B1 decrease following 24-h treatment that is in accordance with a strong G_2-M arrest at this time point (Fig. 3A); densitometric analysis accounted for almost 50% reduction (data not shown). The other important regulator of CDKs is a family of their inhibitory proteins known as CDK inhibitors that bind to CDK-cyclin complex and negatively regulate CDK activity (2, 4). Based on our observed cell cycle arrest effect of gallic acid, we next assessed whether this agent also modulated the levels of CDK inhibitors. As shown in Fig. 3B, treatment of cells with gallic acid resulted in a strong increase in the protein level of Cip1/p21 at 12 and 24 h (~2-fold induction versus control in densitometric analysis; data not shown), without any noticeable changes in Kip1/p27 levels. Together, these results clearly show a decrease in the protein levels of CDKs and cyclins by gallic acid in DU145 cells and a

selective induction in Cip1/p21, suggesting their possible roles in the observed biological responses of gallic acid, including cell cycle arrest.

Effect of Gallic Acid on Cdc25A/Cdc25B/Cdc25C and Cdc2 Levels

In addition to CDKs, cyclins, and CDK inhibitors examined above, the family of cdc25 phosphatases also play an important role specifically in S and G_2-M phases of the cell cycle in which their specific phosphorylation causes their inactivation toward dephosphorylation of cdc2 (CDK1); phosphorylated cdc2 is also inactive in driving cell cycle progression (refs. 22–25 and references therein). Based on our findings showing that gallic acid causes both S and G_2-M arrests, we next assessed its effect on both total and phosphorylated cdc25A, cdc25B, cdc25C, and cdc2 under identical experimental conditions as for other cell cycle regulators. As shown in Fig. 4A, gallic acid treatment of cells resulted in a decrease in total and phosphorylated levels of cdc25C and cdc25A at 12 and 24 h without any effect at early time points on these as well as cdc25B levels; however, a marginal increase in cdc2 phosphorylation without any change in its total level was also observed at early treatment times. Because these results were mostly not consistent with an anticipated increase in cdc25C/cdc25CA followed by cdc2 phosphorylation in terms of their involvement in the observed cell cycle arrest by gallic acid, we next conducted an early time point study. Interestingly, gallic acid treatment of cells resulted in a strong phosphorylation of both cdc25C at Ser^{216} and cdc25A at Ser^{17} as early as 15 min without any changes in their total protein levels (Fig. 4B). The densitometric analyses of these blots showed ~1.8- to 2.9-fold increase in the phosphorylation of cdc25C and cdc25A as a function of time up to 2-h after gallic acid treatment (data not shown). Consistent with these results, gallic acid treatment of cells also showed a strong phosphorylation of cdc2 at Tyr^{15} as early as 15 min without any change in its total protein levels (Fig. 4B). In terms of the quantitative estimation, densitometric analysis of the blot showed 1.3- to 1.7-fold increase in cdc2 phosphorylation at Tyr^{15} as a function of time up to 2 h after gallic acid treatment (data not shown). In other studies (data not shown), gallic acid treatment of cells at all the early time points and up to 24 h as well did not result in any noticeable changes in Wee1, which is a known kinase responsible for cdc2 phosphorylation at Tyr^{15}. Together, these results clearly suggest that gallic acid causes an early inactivating phosphorylation of cdc25C and cdc25A, leading to an accumulation of inactive Tyr^{15}-phosphorylated cdc2, and that these effects of gallic acid possibly drove the observed cell cycle arrest.

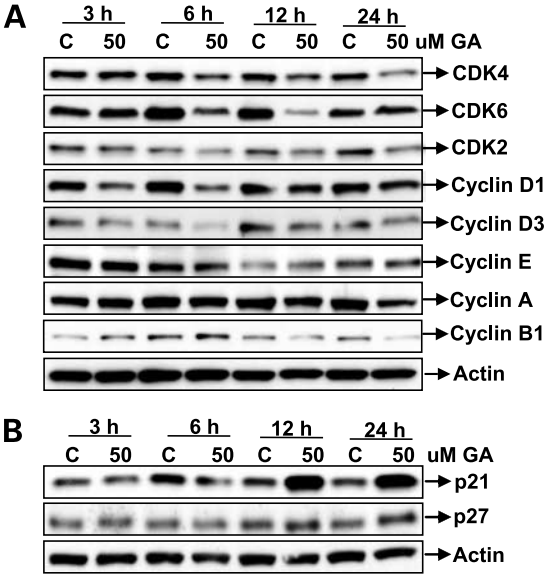

Figure 3. Gallic acid decreases CDKs and cyclins, but induces Cip1/p21 levels in DU145 cells. Cells were cultured as described in Materials and Methods, and treated with either DMSO (control, *C*) or 50 μmol/L gallic acid for 3, 6, 12, and 24 h. At the end of these treatments, total cell lysates were prepared and subjected to SDS-PAGE followed by Western immunoblotting. **A,** for CDKs and cyclins, the membranes were probed with anti-CDK4, CDK6, CDK2, cyclin D1, cyclin D3, cyclin E, cyclin A, cyclin B1, and actin. **B,** for CDK inhibitors, the membranes were probed with anti-Cip1/p21 and Kip1/p27 and actin, antibodies followed by peroxidase-conjugated appropriate secondary antibodies, and visualized by ECL detection system. Representative of at least three independent experiments.

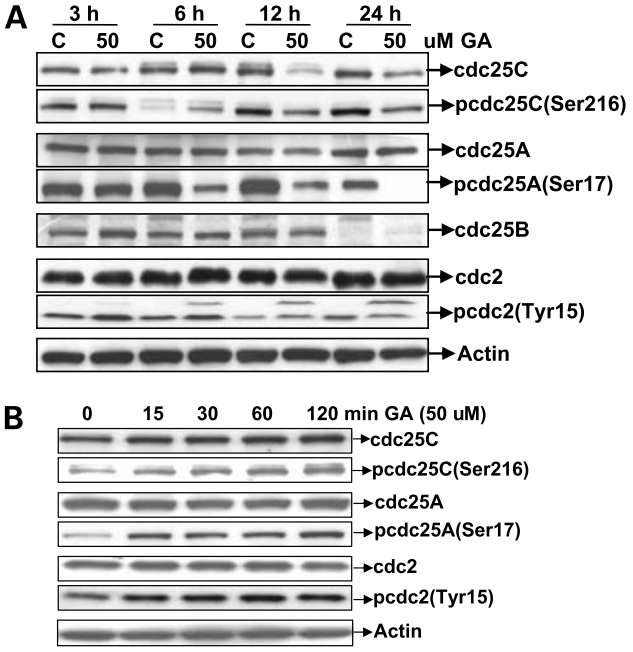

Figure 4. Gallic acid causes phosphorylation of cdc25 phosphatases and cdc2 kinase in DU145 cells. Cells were cultured as described in Materials and Methods, and treated with either DMSO (control) or 50 μmol/L gallic acid for 3, 6, 12, and 24 h (**A**); or 15, 30, 60, and 120 min (**B**). At the end of these treatments, total cell lysates were prepared and subjected to SDS-PAGE followed by Western immunoblotting. The membranes were probed with antibodies for total or phosphorylated (*p*) cdc25C, cdc25A, cdc25B, cdc2, and actin, followed by peroxidase-conjugated appropriate secondary antibodies, and visualized by ECL detection system. Representative of at least three independent experiments.

Effect of Gallic Acid on ATM-Chk2 Activation

Inactivating phosphorylation of cdc25C/A followed by the accumulation of Tyr^{15}-phosphorylated cdc2 and a resultant cell cycle arrest is known to occur via ATM/ATR-Chk1/2 activation in response to DNA damage (refs. 26–29 and references therein). In this regard, ATM and ATR are nuclear kinases recently identified as being activated in response to DNA damage/genotoxic stress in eukaryotic cells (26–29). Based on the results described above, we hypothesized that gallic acid activates ATM/ATR kinases that is known to activate cell cycle checkpoint kinases Chk1/2 (28–30). Accordingly, we next examined the effect of gallic acid on ATM/ATR and Chk1/2 levels and phosphorylation. Gallic acid treatment (50 μmol/L) of cells up to 24 h did not result in any change in total ATR and Chk1 levels as well as Chk1 phosphorylation at any of its known phosphorylation sites (data not shown). However, a strong Chk2 phosphorylation only at Thr^{68} site was observed at 3 and 6 h of gallic acid treatment without any change in its total protein levels (Fig. 5A). Similar to this observation, gallic acid also showed a strong phosphorylation of ATM at Ser^{1981} following its treatment for 3 and 6 h; later time points did not show any effect on both Chk2 and ATM phosphorylation (Fig. 5A). H2A.X is a variant form of histone H2A that is directly phosphorylated at Ser^{139} by an activated ATM kinase, marking an early event in response to DNA damage, and is also known to play a critical role in the retention of DNA repair factors at DNA-damaged sites (31). Because we observed a strong ATM phosphorylation at Ser^{1981} by gallic acid, we also examined the levels of H2A.X phosphorylation at Ser^{139}; we found that, indeed, gallic acid treatment causes strong levels of this effect (Fig. 5A). In additional studies examining whether the time of activation of ATM-Chk2 pathway corroborate the observed phosphorylation of cdc25C/A and accumulation of Tyr^{15}-phosphorylated cdc2, as shown in Fig. 5B, gallic acid treatment caused a strong and a time-dependent increase in the phosphorylation of Chk2 at Thr^{68}, ATM at Ser^{1981}, and H2A.X at Ser^{139}. In other studies, 40 μmol/L gallic acid also showed an increase in the phosphorylation of Chk2, ATM, and H2A.X in an early (15, 30, 60, and 120 min) time kinetics study (data not shown); however, these effects were moderate compared with those observed with 50 μmol/L gallic acid (Fig. 5B).

Gallic Acid – Caused Activation of ATM Leads to Cell Cycle Arrest

The results shown in Figs. 4 and 5 suggested that gallic acid causes a genotoxic stress leading to ATM-Chk2 pathway activation followed by inactivating phosphorylation of cdc25C/A and thereby accumulation of Tyr^{15}-phosphorylated cdc2 in its inactive form as a central mechanism of the observed cell cycle arrest. To further substantiate this suggestion, cells were pretreated with caffeine, which is a known inhibitor of both ATM and ATR

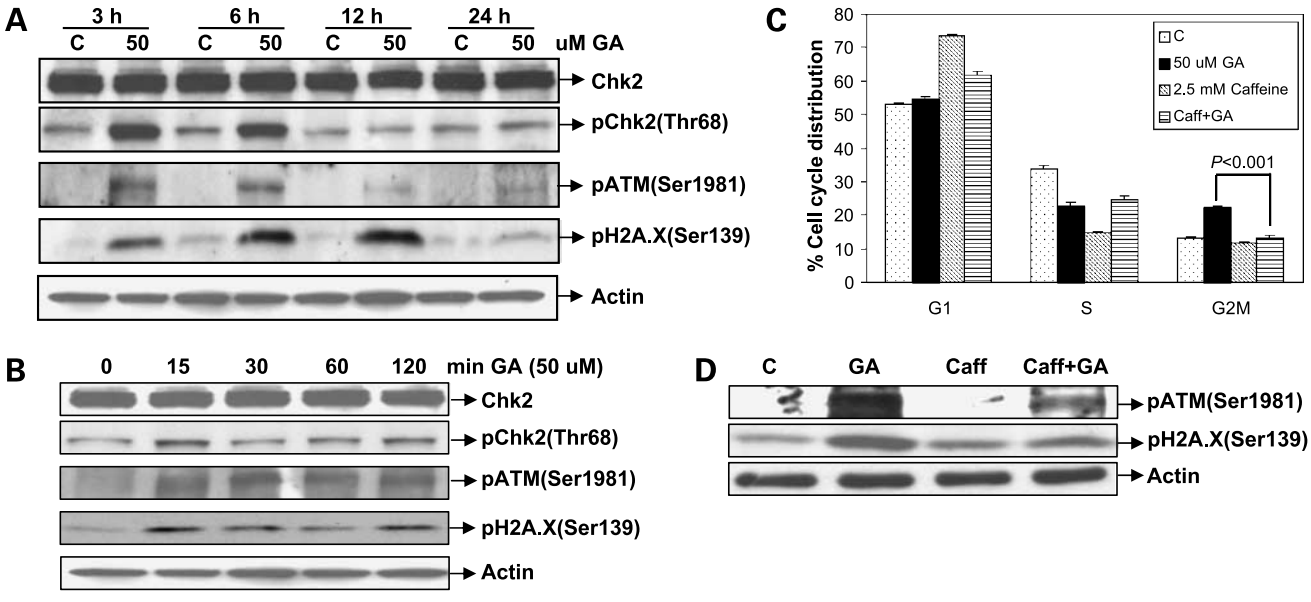

Figure 5. Gallic acid causes phosphorylation of Chk2, ATM, and H2A.X, leading to cell cycle arrest in DU145 cells. Cells were cultured as described in Materials and Methods and treated with either DMSO (control) or 50 μmol/L gallic acid for 3, 6, 12, and 24 h (**A**); or 15, 30, 60, and 120 min (**B**). At the end of these treatments, total cell lysates were prepared and subjected to SDS-PAGE followed by Western immunoblotting. The membranes were probed with antibodies for total or phosphorylated Chk2, ATM, H2A.X, and actin, followed by peroxidase-conjugated appropriate secondary antibodies, and visualized by ECL detection system. Representative of at least three independent experiments. In other studies, DU145 cells were treated with DMSO (control), caffeine (*Caff*, 2.5 mmol/L) alone, or 50 μmol/L gallic acid without or with 2-h pretreatment with caffeine (2.5 mmol/L) for 24 h (**C**) or 3 h (**D**). At the end of these treatments, cells were harvested and analyzed for cell cycle distribution as detailed in Materials and Methods (**C**), or cells were harvested and cell lysates were prepared and subjected to SDS-PAGE followed by Western immunoblotting for phospho-ATM, phospho-H2A.X, and actin (**D**). *Columns,* mean of triplicate samples; *bars,* SE. Cell cycle data were reproducible in an additional independent experiment. The immunoblot results are representative of two independent experiments.

kinases (32), and then the effect of gallic acid on cell cycle progression and associated upstream events was examined. Pretreatment of cells with caffeine completely reversed gallic acid, induced G_2-M arrest ($P < 0.001$) observed following 24 h of its treatment (Fig. 5C), and strongly reduced gallic acid caused phosphorylation of both ATM and H2A.X (Fig. 5D). Together, these findings suggest that gallic acid causes DNA damage leading to ATM activation followed by Ser^{139} phosphorylation of H2A.X, supporting the role of ATM activation in cell cycle arrest by gallic acid.

Gallic Acid Causes Both Caspase-Dependent and Caspase–Independent Apoptotic Cell Death

Based on our results showing that gallic acid causes strong apoptotic death (Fig. 2D), studies were also done to examine whether caspase activation is involved in this effect of gallic acid. As shown in Fig. 6A, treatment of cells with gallic acid resulted in a time-dependent increase in caspase-9, caspase-3, and poly(ADP)ribose polymerase cleavage with strongest effect at 24 h, suggesting a possible involvement of caspase activation in the apoptotic effect of gallic acid. To further address this issue, cells were pretreated with pan-caspase inhibitor ZVAD.fmk followed by gallic acid, and quantitative apoptotic cell population was measured. Interestingly, compared with gallic acid alone, pretreatment with caspase inhibitor resulted in more apoptotic cell death (Fig. 6B). To substantiate that caspase activation is indeed inhibited by caspase inhibitor pretreatment, under similar experimental conditions, samples were also analyzed for cleaved caspase-9 and cleaved caspase-3, which showed a complete reversal in their activation (Fig. 6C), suggesting that, at least under caspase-inhibiting conditions, additional pathway(s) is involved in the apoptotic effects of gallic acid. More studies are needed in the future to define both caspase-dependent and caspase-independent mechanisms of gallic acid–caused apoptotic cell death, and to address whether caspase activation initiates apoptosis or is part of terminal processing of death.

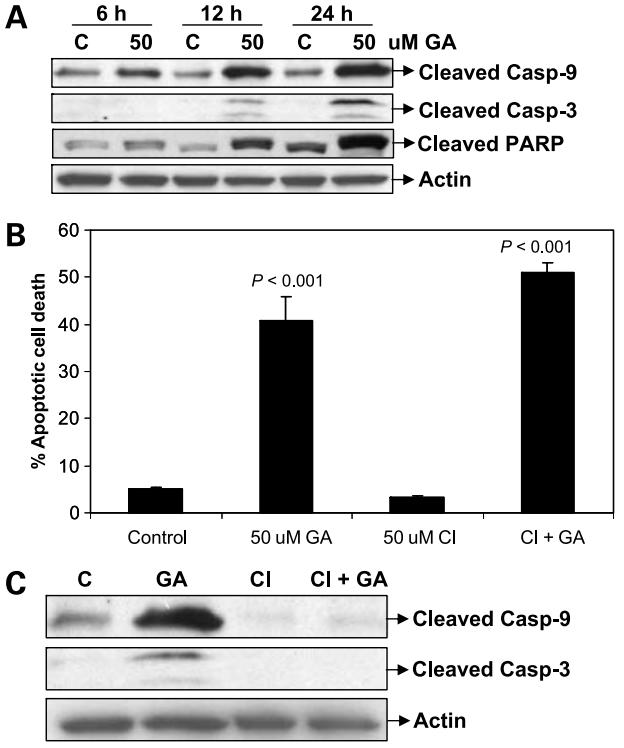

Figure 6. Gallic acid causes both caspase-dependent and caspase-independent apoptotic cell death. **A,** DU145 cells were treated with either DMSO (control) or 50 μmol/L gallic acid for 6, 12, and 24 h, and total cell lysates were prepared and subjected to SDS-PAGE followed by Western immunoblotting. The membranes were probed with antibodies for cleaved caspase-9, caspase-3, and poly(ADP)ribose polymerase, and actin followed by peroxidase-conjugated appropriate secondary antibodies, and visualized by ECL detection system. Representative of two independent experiments. In other studies, cells were treated with either DMSO (control) or 50 μmol/L gallic acid without or with 2-h pretreatment with pan–caspase inhibitor ZVAD.fmk (*CI*, 50 μmol/L), or CI alone for 24 h. At the end of these treatments, cells were harvested and analyzed for apoptotic cell death as detailed in Materials and Methods (**B**), or cells were harvested and cell lysates were prepared and subjected to SDS-PAGE followed by Western immunoblotting for cleaved caspase-9 and caspase-3, and actin (**C**). *Columns,* mean of triplicate samples; *bars,* SE. The data for percentage of apoptotic cell death were reproducible in an additional independent experiment. The immunoblot results shown are representative of two independent experiments.

Discussion

A wide range of naturally occurring substances have been shown to protect against experimental carcinogenesis, and numerous studies in the literature suggest that phytochemicals, particularly those in our daily diet, possess strong anticancer and cancer chemopreventive properties against various malignancies, including prostate cancer (refs. 3, 5, 6, 33–35 and references therein). In this regard, gallic acid is a ubiquitous dietary phytochemical being present in virtually all the fruits and vegetables, as well as in beverages such as green tea and red wine, either in its free or esterified forms (refs. 36, 37 and references therein). However, only few studies have shown the anticancer activity of gallic acid in limited cancer cell lines, including a study showing its selective cell death effect in various human and rodent cancer cells but not in normal cells (38, 39). With regard to prostate cancer, our study for the first time reports the biological activity of gallic acid in prostate cancer DU145 cells and associated mechanisms of its efficacy.

The central findings of the present study are that via ATM-Chk2 activation, gallic acid causes inactivating phosphorylation of cdc25C/A phosphatases, leading to accumulation of cdc2 in its Tyr^{15}-phosphorylated inactive form and a resultant cell cycle arrest. Inhibition of ATM kinase by its specific inhibitor caffeine abrogated gallic acid–caused phosphorylation of both ATM and H2A.X and reversed gallic acid–induced cell cycle arrest, further supporting the role of gallic acid–caused DNA damage and ATM activation in its cell cycle arrest activity. Many DNA-damaging agents, especially those that generate DNA double-strand breaks, are known to activate ATM kinase and induce ATM-dependent apoptosis (22). Histone H2A.X, one of the target proteins of ATM, is phosphorylated by activated ATM at Ser^{139} (31). In the present

study, we also observed that gallic acid induces Ser^{139} phosphorylation of H2A.X in DU145 cells, which is inhibited by caffeine, suggesting the involvement of ATM activation in gallic acid–induced DNA damage signaling.

The checkpoint functions of ATM and ATR are mediated by checkpoint effector kinases known as Chk1 and Chk2 (40), which are structurally distinct but functionally related kinases that phosphorylate an overlapping pool of cellular substrates (41). In mammalian cells, it has been shown that Chk1 and Chk2 play a central role in transducing DNA damage signals from ATR and ATM, respectively, in which Chk1 seems to be activated by ATR in response to replication inhibition and UV-induced damage, whereas Chk2 primarily functions through ATM in response to ionizing radiation (23, 42). The activation of Chk2 in response to DNA damage requires its phosphorylation at Thr^{68} (43, 44). Accordingly, our data is consistent with other emerging information on the phosphorylation of Chk2 by ATM. For example, gallic acid treatment did not show any effect on ATR levels and also did not cause the phosphorylation of Chk1 at any of its known sites (data not shown). However, gallic acid showed a strong ATM activation in terms of its phosphorylation at Ser^{1981}, together with Chk2 phosphorylation at Thr^{68} as well as that of H2A.X at Ser^{139}. Furthermore, the time kinetics of these effects of gallic acid was also consistent, suggesting a close association between these events following gallic acid treatment of DU145 cells.

Activation of Chk1 and/or Chk2 causes the phosphorylation and thereby inactivation of cdc25 family of tyrosine phosphatases, which creates a binding site for 14-3-3 proteins and results in their export to and retention in the cytoplasm (45, 46). Nuclear cdc2 remains phosphorylated in the absence of active cdc25 phosphatases, and the cells remain arrested in specific phase. During S and G_2 phases of the cell cycle, the cdc2-cyclin B complex is kept in the inactive state through Tyr^{15} phosphorylation of cdc2 by Wee1/Mik1/Myt1 tyrosine kinases (32, 33); however, during the G_2-M transition, cdc2 is rapidly converted into the active form by Tyr^{15} dephosphorylation catalyzed by cdc25 tyrosine phosphatases (47, 48). Increased levels of Tyr^{15}-phosphorylated cdc2 have been shown to be associated with cell cycle arrest following DNA damage in many cell culture systems (42, 49). Consistent with these reports and with the activation of ATM-Chk2 by gallic acid, our results also show that gallic acid induces the inactivating phosphorylation of cdc25C (Ser^{216}) and cdc25A (Ser^{17}). Moreover, as a downstream effect, Tyr^{15}-phosphorylated cdc2 did not get dephosphorylated by cdc25 phosphatases, keeping cdc2 (Tyr^{15}) in an inactive form that leads to a resultant cell cycle arrest. In summary, the present study identifies gallic acid efficacy and associated mechanisms in an advanced and androgen-independent human prostate carcinoma DU145 cells, suggesting future *in vivo* efficacy studies with this ubiquitous dietary agent in preclinical prostate cancer models.

References

1. Jemal A, Siegel R, Ward E, et al. Cancer statistics, 2006. CA Cancer J Clin 2006;56:106 – 30.

2. Agarwal R. Cell signaling and regulators of cell cycle as molecular targets for prostate cancer prevention by dietary agents. Biochem Pharmacol 2000;60:1051 – 9.

3. Singh RP, Agarwal R. Natural flavonoids targeting deregulated cell cycle progression in cancer cells. Curr Drug Targets 2006;7:345 – 54.

4. Singh RP, Agarwal R. Mechanisms of action of novel agents for prostate cancer chemoprevention. Endocrine-related cancer, published online on June 1, 2006. http://intl-erc.endocrinology-journals.org.

5. Surh YJ. Cancer chemoprevention with dietary phytochemicals. Nat Rev Cancer 2003;3:768 – 80.

6. Nelson WG, Wilding G. Prostate cancer prevention agent development: criteria and pipeline for candidate chemoprevention agents. Urology 2001; 57:56 – 63.

7. Packer L, Rimbach G, Virgili, F. Antioxidant activity and biologic properties of a procyanidin-rich extract from pine (*Pinus maritima*) bark, pycnogenol. Free Radic Biol Med 1999;27:704 – 24.

8. Maffei Facino R, Carini M, Aldini G, et al. Procyanidines from *Vitis vinifera* seeds protect rabbit heart from ischemia/reperfusion injury: antioxidant intervention and/or iron and copper sequestering ability. Planta Med 1996;62:495 – 502.

9. Ferreira D, Slade D. Oligomeric proanthocyanidins: naturally occurring O-heterocycles. Nat Prod Rep 2002;19:517 – 41.

10. Ye X, Krohn RL, Liu W, et al. The cytotoxic effects of a novel IH636 grape seed proanthocyanidin extract on cultured human cancer cells. Mol Cell Biochem 1999;196:99 – 108.

11. Agarwal C, Sharma Y, Zhao J, Agarwal R. A polyphenolic fraction from grape seeds causes irreversible growth inhibition of breast carcinoma MDA-MB468 cells by inhibiting mitogen-activated protein kinases activation and inducing G1 arrest and differentiation. Clin Cancer Res 2000;6: 2921 – 30.

12. Tyagi A, Agarwal R, Agarwal C. Grape seed extract inhibits EGF-induced and constitutively active mitogenic signaling but activates JNK in human prostate carcinoma DU145 cells: possible role in anti-proliferation and apoptosis. Oncogene 2003;22:1302 – 16.

13. Agarwal C, Singh RP, Agarwal R. Grape seed extract induces apoptotic death of human prostate carcinoma DU145 cells via caspases activation accompanied by dissipation of mitochondrial membrane potential and cytochrome *c* release. Carcinogenesis 2002;23:1869 – 76.

14. Kaur M, Agarwal R, Agarwal C. Grape Seed Extract induces anoikis and caspase-mediated apoptosis in human prostate carcinoma LNCaP cells: possible role of ATM-p53 activation. Mol Cancer Ther 2006;5:1265 – 74.

15. Singletary KW, Meline B. Effect of grape seed proanthocyanidins on colon aberrant crypts and breast tumors in a rat dual-organ tumor model. Nutr Cancer 2001;39:252 – 8.

16. Nomoto H, Iigo M, Hamada H, Kojima S, Tsuda H. Chemoprevention of colorectal cancer by grape seed proanthocyanidin is accompanied by a decrease in proliferation and increase in apoptosis. Nutr Cancer 2004;49: 81 – 8.

17. Bomser JA, Singletary KW, Wallig MA, Smith MAL. Inhibition of TPA-induced tumor promotion in CD-1 mouse epidermis by a polyphenolic fraction from grape seeds. Cancer Lett 1999;135:151 – 7.

18. Zhao J, Wang J, Chen Y, Agarwal R. Anti-tumor promoting activity of a polyphenolic fraction isolated from grape seeds in mouse skin two-stage initiation-promotion protocol, and identification of procyanidin B5-3′-gallate as the most effective antioxidant constituent. Carcinogenesis 1999;20:1737 – 45.

19. Mittal A, Elmets CA, Katiyar SK. Dietary feeding of proanthocyanidins from grape seeds prevents photocarcinogenesis in SKH-1 hairless mice: relationship to decreased fat and lipid peroxidation. Carcinogenesis 2003; 24:1379 – 88.

20. Singh RP, Tyagi AK, Dhanalakshmi S, Agarwal R, Agarwal C. Grape seed extract inhibits advanced human prostate tumor growth and angiogenesis and upregulates insulin-like growth factor binding protein-3. Int J Cancer 2004;108:733 – 40.

21. Veluri R, Singh RP, Liu Z, Thompson JA, Agarwal R, Agarwal C. Fractionation of grape seed extract and identification of gallic acid as one of the major active constituents causing growth inhibition and apoptotic death of DU145 human prostate carcinoma cells. Carcinogenesis 2006; 27:1445 – 53.

22. Zhou BB, Elledge SJ. The DNA damage response: putting checkpoints in perspective. Nature 2000;408:433 – 9.

23. Bulavin DV, Higashimoto Y, Demidenko ZN, et al. Dual phosphorylation controls Cdc25 phosphatases and mitotic entry. Nat Cell Biol 2003; 6:545 – 51.

24. Jin P, Gu Y, Morgan DO. Role of inhibitory CDC2 phosphorylation in radiation-induced G_2 arrest in human cells. J Cell Biol 1996;134: 963 – 70.

25. Singh SV, Herman-Antosiewicz A, Singh AV, et al. Sulforaphane-induced G_2/M phase cell cycle arrest involves checkpoint kinase 2-mediated phosphorylation of cell division cycle 25C. J Biol Chem 2004; 279:25813 – 22.

26. Kastan MB, Lim DS. The many substrates and functions of ATM. Nat Rev Mol Cell Biol 2000;1:179 – 86.

27. Abraham RT. Cell cycle checkpoint signaling through the ATM and ATR kinases. Genes Dev 2001;15:2177 – 96.

28. Shiloh Y. ATM and related protein kinases: safeguarding genome integrity. Nat Rev Cancer 2003;3:155 – 68.

29. Khanna KK, Lavin MF, Jackson SP, Mulhern TD. ATM, a central controller of cellular responses to DNA damage. Cell Death Differ 2001;8: 1052 – 65.

30. Matsuoka S, Huang M, Elledge SJ. Linkage of ATM to cell cycle regulation by the Chk2 protein kinase. Science 1998;282:1893 – 7.

31. Burma S, Chen BP, Murphy M, Kurimasa A, Chen DJ. ATM phosphorylates histone H2AX in response to DNA double-strand breaks. J Biol Chem 2001;276:42462 – 7.

32. Sarkaria JN, Busby EC, Tibbetts RS, et al. Inhibition of ATM and ATR kinase activities by the radiosensitizing agent, caffeine. Cancer Res 1999; 59:4375 – 82.

33. Park EJ, Pezzuto JM. Botanicals in cancer chemoprevention. Cancer Metastasis Rev 2002;21:231 – 55.

34. Bemis DL, Capodice JL, Costello JE, Vorys GC, Katz AE, Buttyan R. The use of herbal and over-the-counter dietary supplements for the prevention of prostate cancer. Curr Oncol Rep 2006;8:228 – 36.

35. Klein EA. Chemoprevention of prostate cancer. Annu Rev Med 2006; 57:49 – 63.

36. Hour TC, Liang YC, Chu IS, Lin JK. Inhibition of eleven mutagens by various tea extracts, (−)epigallocatechin-3-gallate, gallic acid and caffeine. Food Chem Toxicol 1999;37:569 – 79.

37. Haslam E, Cai Y. Plant polyphenols (vegetable tannins): gallic acid metabolism. Nat Prod Rep 1994;11:41 – 66.

38. Inoue M, Suzuki R, Sakaguchi N, et al. Selective induction of cell death in cancer cells by gallic acid. Biol Pharm Bull 1995;18:1526 – 30.

39. Gomes CA, da Cruz TG, Andrade JL, Milhazes N, Borges F, Marques MP. Anticancer activity of phenolic acids of natural or synthetic origin: a structure-activity study. J Med Chem 2003;46:5395 – 401.

40. Khanna KK, Jackson SP. DNA double-strand breaks: signaling, repair and the cancer connection. Nat Genet 2001;27:247 – 54.

41. O'Neill T, Giarratani L, Chen P, et al. Determination of substrate motifs for human Chk1 and hCds1/Chk2 by the oriented peptide library approach. J Biol Chem 2002;277:16102 – 15.

42. Zhao H, Piwnica-Worms H. ATR-mediated checkpoint pathways regulate phosphorylation and activation of human Chk1. Mol Cell Biol 2001;21:4129 – 39.

43. Ahn JY, Schwarz JK, Piwnica-Worms H, Canman CE. Threonine 68 phosphorylation by ataxia telangiectasia mutated is required for efficient activation of Chk2 in response to ionizing radiation. Cancer Res 2000;60: 5934 – 6.

44. Matsuoka S, Rotman G, Ogawa A, Shiloh Y, Tamai K, Elledge SJ. Ataxia telangiectasia-mutated phosphorylates Chk2 *in vivo* and *in vitro*. Proc Natl Acad Sci U S A 2000;97:10389 – 94.

45. Lopez-Girona A, Furnari B, Mondesert O, Russell P. Nuclear localization of Cdc25 is regulated by DNA damage and a 14-3-3 protein. Nature 1999;397:172 – 5.

46. Peng CY, Graves PR, Thoma RS, Wu Z, Shaw AS, Piwnica-Worms H. Mitotic and G_2 checkpoint control: regulation of 14-3-3 protein binding by phosphorylation of Cdc25C on serine-216. Science 1997;277: 1501 – 5.

47. Russell P, Nurse P. The mitotic inducer $nim1^+$ functions in a regulatory network of protein kinase homologs controlling the initiation of mitosis. Cell 1987;49:569 – 76.

48. Kumagai A, Dunphy WG. The cdc25 protein controls tyrosine dephosphorylation of the cdc2 protein in a cell-free system. Cell 1991; 64:903 – 14.

49. Barth H, Hoffmann I, Klein S, Kaszkin M, Richards J, Kinzel V. Role of cdc25-C phosphatase in the immediate G_2 delay induced by the exogenous factors epidermal growth factor and phorbol ester. J Cell Physiol 1996;168:589 – 99.